Gene Expression, Vol. 17, pp. 327–340
Printed in the USA.

1052-2166/17 $90.00 + .00
DOI: https://doi.org/10.3727/105221617X15042723767876
E-ISSN 1555-3884
www.cognizantcommunication.com

The Cholangiocyte Adenosine–IL-6 Axis Regulates Survival During Biliary Cirrhosis

Elise G. Lavoie,*† Michel Fausther,*† Jessica R. Goree,*† and Jonathan A. Dranoff*†

*Division of Gastroenterology and Hepatology, University of Arkansas for Medical Sciences, Little Rock, AR, USA
†Research Service, Central Arkansas VA Healthcare System, Little Rock, AR, USA

Epithelial response to injury is critical to the pathogenesis of biliary cirrhosis, and IL-6 has been suggested as a mediator of this phenomenon. Several liver cell types can secrete IL-6 following activation by various signaling molecules including circulating adenosine. The aims of this study were to assess whether adenosine can induce IL-6 secretion by cholangiocytes via the A2b adenosine receptor (A2bAR) and to determine the effect of A2bAR-sensitive IL-6 release on injury response in biliary cirrhosis. Human normal cholangiocyte H69 cells were used for in vitro studies to determine the mechanism by which adenosine and the A2bAR induce release of IL-6. In vivo, control and A2bAR-deficient mice were used to determine the roles of A2bAR-sensitive IL-6 release in biliary cirrhosis induced by common bile duct ligation (BDL). Additionally, the response to exogenous IL-6 was assessed in C57BL/6 and A2bAR-deficient mice. Adenosine induced IL-6 mRNA expression and protein secretion via A2bAR activation. Although activation of A2bAR induced cAMP and intracellular Ca^{2+} signals, only the Ca^{2+} signals were linked to IL-6 upregulation. After BDL, A2bAR-deficient mice have impaired survival, which is further impaired by exogenous IL-6; however, decreased survival is not due to changes in fibrosis and no changes in inflammatory cells. Exogenous IL-6 is associated with the increased presence of bile infarcts. Extracellular adenosine induces cholangiocyte IL-6 release via the A2bAR. This signaling pathway is important in the pathogenesis of injury response in biliary cirrhosis but does not alter fibrosis. Adenosine upregulates IL-6 release by cholangiocytes via the A2bAR in a calcium-sensitive fashion. Mice deficient in A2bAR experience impaired survival after biliary cirrhosis induced by common bile duct ligation independent of changes in fibrosis.

Key words: Adenosine; Interleukin-6 (IL-6); Adenosine receptor; Cholangiocyte; Liver fibrosis; Biliary cirrhosis

INTRODUCTION

The liver is unique in its capacity for regeneration. While regeneration can restore function after acute liver injury or removal of parenchyma, regeneration is also a critical component of cirrhosis[1,2]. Few signals have been linked to both regenerative injury response and cirrhosis progression; however, published data suggest that interleukin-6 (IL-6) may act as one such signal[3,4].

IL-6 is a cytokine released following inflammation or tissue damage. IL-6 has potent pro- and anti-inflammatory effects mediated by the activation of both transmembrane (IL-6R and gp80) and soluble (sIL-6R) receptors[5,6]. In the liver, IL-6 is known to be an activator of acute phase response genes[7] and a promoter of hepatocyte[3,8] and cholangiocyte[9] proliferation.

Several lines of evidence suggest that IL-6 is important in liver regeneration. The serum concentration of IL-6 increases following partial hepatectomy (PH)[10,11]. Also, IL-6-deficient mice that underwent PH have higher death rates and decreased hepatocyte proliferative indices compared to wild-type animals[12–14]. That phenotype can be completely reversed when exogenous IL-6 is given to IL-$6^{-/-}$ mice prior to PH[13,14]. On the other hand, IL-6 may actually ameliorate injury in biliary cirrhosis. Animals deficient in IL-6 develop higher total serum bilirubin levels and have higher mortality rates than wild-type counterparts, when subjected to bile duct ligation for up to 12 weeks[15].

In the liver, the major sources of IL-6 are Kupffer cells[16,17], liver sinusoidal endothelial cells[18], and cholangiocytes[9,19–21]. IL-6 secretion may be induced by factors such as lipopolysaccharide (LPS), tumor necrosis factor-α (TNF-α), IL-1β,[4,5] or estrogen[21]. Most relevant to the studies shown in this article, extracellular adenosine can

Address correspondence to Jonathan A. Dranoff, M.D., University of Arkansas for Medical Sciences, 4301 West Markham Street #567, Little Rock, AR 72205, USA. Tel: +1-501-686-7840; Fax: +1-501-686-6248; E-mail: jadranoff@uams.edu

activate IL-6 release via the activation of the A2b adenosine receptor (A2bAR)[22–24].

The circulating nucleoside adenosine derives primarily from the degradation of the nucleotide adenosine triphosphate (ATP), which is released in the extracellular environment both in regulated fashion[25] and after plasma membrane disruption due to cell injury or death[26–28]. Sequential hydrolysis of extracellular ATP to adenosine is catalyzed by a number of cell surface enzymes, including ectonucleoside triphosphate diphosphohydrolases[29,30] and ecto-5′-nucleotidase[31]. Once generated, extracellular adenosine may activate the four members of the adenosine seven-transmembrane domain receptor (AR) family: A1, A2a, A2b, and A3AR[32]. A1AR, A2aAR, and A3AR are high-affinity receptors that respond to low concentrations (>10 nM) of extracellular adenosine, while A2bAR (>1 μM) is a low-affinity receptor that will only be activated in pathological conditions[33]. A2bAR is also unique in its signal transduction, since it is linked to both G_q- and G_s-coupled second messengers[34].

Since the enzymes necessary for the biochemical conversion of ATP to adenosine are expressed in the liver[35] and regulated by injury[35,36], we tested the hypothesis that extracellular adenosine activates A2bAR signaling pathways within cholangiocytes, mediating IL-6 secretion, which is ultimately relevant to injury response in the setting of biliary fibrosis/cirrhosis. In this article, we examined this concept via a series of in vitro and in vivo experiments.

MATERIALS AND METHODS

Materials

Cell culture reagents and media were obtained from Invitrogen (Life Technologies Corporation, Grand Island, NY, USA). Antibodies used in this study are as follows: polyclonal rabbit anti-Ki-67 antibody (Abcam, Cambridge, MA, USA), polyclonal rabbit anti-A2bAR antibody (Alomone Labs, Jerusalem, Israel), monoclonal rat anti-mouse neutrophil antibody (NIMP-R14; Abcam), monoclonal rat anti-mouse F4/80 (Cl:A3-1; Bio-Rad Laboratories, Hercules, CA), and monoclonal rabbit anti-CD3 (SP7; Abcam). The monoclonal rat anti-cytokeratin-19 (CK19) antibody (TROMA-III) developed by Rolf Kemler (Max-Planck Institute, Freiburg, Germany) was obtained from the Developmental Studies Hybridoma Bank developed under the auspices of the NICHD and maintained by the Department of Biology, University of Iowa (Iowa City, IA, USA).

Animal Use

All procedures were performed in agreement with the guidelines approved by the Institutional Animal Care and Use Committee of the University of Arkansas for Medical Sciences (UAMS). $A2bAR^{-/-}$ mice[37] were provided by Dr. Katya Ravid (Boston University School of Medicine, Boston, MA, USA). C57BL/6 mice were obtained from the Charles River Laboratory (Oak Forest, AR, USA). Age-matched male $A2bAR^{-/-}$ and C57BL/6 mice (8 to 14 weeks old) were used in all experiments. All mice that underwent survival surgery were given subcutaneous injection of buprenorphine (0.1 mg/kg) every 12 h for the next 48 h as needed. In addition, ibuprofen (Perrigo, Allegan, MI, USA) was given ad libitum in the drinking water for 48 h following surgery.

Bile Duct Ligation (BDL)

BDL surgeries were performed as previously described[38]. For some experiments, $A2bAR^{-/-}$ and C57BL/6 mice were injected subcutaneously with 250 ng/g of body weight of mouse recombinant IL-6 (recmIL-6; BioLegend, San Diego, CA, USA) or vehicle 15 min prior to the surgery and once a week for the duration of the experiments.

At the end of the experiments, mice were anesthetized with ketamine/xylazine before blood samples were collected from the vena cava for serum collection following centrifugation, and livers were resected. One lobe was fixed in 10% neutral-buffered formalin and embedded in paraffin for histological analysis. Sections of liver were flash frozen in dry ice-cooled isopentane for protein isolation or placed in RNAlater solution (Live Technology) for RNA isolation.

Cell Culture, Transfection, and Stimulation

Immortalized human normal cholangiocyte H69 cells were provided by Dr. Doug Jefferson (Tufts University School of Medicine, Boston, MA, USA) and cultured as previously described[39]. For siRNA experiments, H69 cells were plated at 300,000 cells in T25 flasks the day before transfection. The cells were transfected with 250 pm of nontargeting (scramble control) or targeting (specific) human A2bAR On-TARGET plus siRNA smartpools (GE Healthcare Dharmacon, Lafayette, CO, USA) with Lipofectamine 2000 (Life Technologies, Carlsbad, CA, USA) following the manufacturer's instructions. When required, cells were trypsinized 24 h posttransfection and counted before plating in appropriate multiwell plate format for further experiments. Transfected and non-transfected cells were stimulated with adenosine (Tocris Bioscience, Minneapolis, MN, USA) and 5′-*N*-ethylcarboxamidoadenosine (NECA[40]; Tocris Bioscience) for 2 h (qPCR and cAMP ELISA) or 4 h (IL-6 ELISA) +/−: selective A2bAR antagonist MRS-1754 (1 μM[41]; Tocris Bioscience), calcium chelator BAPTA/AM (50 μM; Life Technologies) cyclic AMP analog acting as an inhibitor of cAMP-dependent protein kinase, (*R*)-adenosine, cyclic 3′,5′-(hydrogenphosphorothioate) triethylammonium (cAMPS-RP; 100 μM; Tocris Bioscience). H69 cells were

Table 1. List of the Semiquantitative Primer Sequences Used in the Study

Genes	Sequences 5′–3′
Human ADORA1 (Accession No. NM_000674)	Forward: CCT CCA TCT CAG CTT TCC AG Reverse: AGT AGG TCT GTG GCC CAA TG
Human ADORA2a (Accession No. NM_000675)	Forward: AAC CTG CAG AAC GTC ACC AA Reverse: GTC ACC AAG CCA TTG TAC CG
Human ADORA2b (Accession No. NM_000676.2)	Forward: GAG ACA CAG GAC GCG CTG TAC G Reverse: CGG GTC CCC GTG ACC AAA CT
Human ADORA3 variants 1 and 3 (Accession No. NM_0020683 and NM_001081976)	Forward: GAC ACA GGG AAC CAG CTC AT Reverse: TGC AGC TTC TGG TTT TGT TG
Human ADORA3 variant 2 (Accession No. NM_000677)	Forward: TGT TTG GCT GGA ACA TGA AA Reverse: ATA GAT GGC GCA CAT GAC AA
Human ACTB (Accession No. NM_001101.3)	Forward: GCG AGA AGA TGA CCC AGA TC Reverse: CCA GTG GTA CGG CCA GAG G
Human GAPDH (Accession No. NM_002046.5)	Forward: TCA CCA TCT TCC AGG AG Reverse: GCT TCA CCA CCT TCT TG

also stimulated with the exchange protein directly activated by cAMP (EPAC) activator 8-(4-chlorophenylthio)-2′-*O*-methyladenosine-3′,5′-cyclic monophosphate acetoxymethyl ester (8-pCPT-2-O-Me-cAMP-AM; Tocris Bioscience). For pharmacological inhibition, cells were preincubated for 30 min with the antagonist(s) before changing media for agonist-containing media. Cells were used for analysis 72 h after siRNA transfection. RNA was extracted from transfected cells, and A2bAR downregulation was confirmed by qPCR as described below.

Qualitative and Quantitative RT-PCR

H69 cholangiocyte RNA was extracted with the RNeasy Plus Extraction Kit according to the manufacturer's instructions (Qiagen, Valencia, CA, USA). RNA concentration was determined with the Qubit system following the manufacturer's instruction (Life Technologies). RNA (1 μg) was treated with DNase1 (Ambion, Life Technologies) before reverse transcription with the iScript Reverse Transcriptase Kit (Bio-Rad Laboratories). gDNA contamination was assessed by examining β-actin (*ACTB*) or glyceraldehyde 3-phosphate dehydrogenase (*GAPDH*) PCR on the no-reverse transcriptase reaction. RT-PCRs were performed with the TopTaq PCR Master Mix (Qiagen). PCR conditions were as follows: initialization at 94°C for 2 min followed by 35 cycles of 30 s of denaturation at 94°C, 30 s of annealing at 60°C (*ACTB* or *GAPDH*) or 62°C (adenosine receptors), and 30 s of elongation at 72°C; the amplification was then completed with a 10-min final elongation at 72°C using an S1000 Thermal Cycler (Bio-Rad). All primer sequences used in the study are listed in the Table 1. For qRT-PCR, *ADORA2b*, *IL-6*, mRNA expression was quantified by relative quantitative real-time PCR (qPCR) using the CFX96 thermocycler (Bio-Rad) with the SSoFast or SSoAdvance qPCR master mixes (Bio-Rad). β-2-microglobulin (*B2M*), *GAPDH*, and hypoxanthine rhosphoribosyl transferase-1 (*HPRT1*) were used as genes of references. Gene-specific probes (PrimeTime qPCR assay, see Table 2 for probe reference number) were obtained from Integrated DNA Technology (Coralville, IA, USA).

ELISA

cAMP. Cells were stimulated in 96-well plates as described above. Intracellular cAMP was measured using the Amersham cAMP Biotrack enzyme immunoassay (EIA) system (GE Healthcare Life Sciences, Piscataway, NJ, USA) according to the manufacturer's instructions.

Human IL-6. Cells were stimulated in 48-well plates as described above. Supernatants were collected, centrifuged to removed cell debris, and kept at −80°C for further analysis. IL-6 concentrations were determined by ELISA using the Human IL-6 Quantikine ELISA Kit (R&D Systems, Minneapolis, MN, USA) according to the manufacturer's instructions.

Mouse IL-6. Sera were collected as described above. Serum IL-6 concentrations were determined by ELISA

Table 2. List of the qPCR Probes Used in the Study

Genes	Accession Nos.	IDT Probe Nos.
ADORA2b	Human: NM_000676	Hs.PT.47.4289481
IL-6	Human: NM_000600	Hs.PT.53a.3074634
	Mouse: NM_031168	Mm.PT.56a.10005566
GAPDH	Human: NG_007073.2	Hs.PT.39a.22214836
	Mouse: NM_008084	Mm.PT.39a.1
B2M	Human: NM_004048	Hs.PT.39a.22214845
	Mouse: NM_009735	Mm.Pt.39a.22214835
HPRT	Human: NM_000194	Hs.PT.39a.22214821
	Mouse: NM_013556	Mm.PT.39a.22214828

using the mouse IL-6 quantikine ELISA kit (R&D Systems) according to the manufacturer's instructions.

Immunofluorescence

H69 cholangiocytes were plated on glass coverslips before staining. Following fixation with 4% paraformaldehyde for 15 min at room temperature, cells were blocked in a solution of 7% (v/v) goat serum and 0.5% (w/v) bovine serum albumin (BSA) in 1× phosphate-buffered saline (PBS) buffer and incubated overnight with a polyclonal rabbit anti-human A2bAR antibody (dilution 1:100 in blocking solution; Alomone Laboratories) followed by a 1-h incubation with an Alexa Fluor 488-conjugated goat anti-rabbit IgG secondary antibody (dilution 1:1,000; Life Technologies). After the final washing steps with 1× PBS and water, coverslips were mounted on glass slides with ProLong gold with DAPI (Life Technologies).

Confocal Video Microscopy

For intracellular Ca^{2+} mobilization imaging, H69 cholangiocytes were plated on glass coverslips and loaded with the cell-permeant Ca^{2+}-sensitive fluorophore Fluo-4/AM (Life Technologies). Coverslips were transferred into a specially designed apparatus allowing perifusion with buffer onto the stage of a Zeiss LSM Meta 510 microscope (Zeiss, Thornwood, NY, USA). Initially, cells were perifused to equilibrium at a constant rate with 2-[4-(2-hydroxyethyl)piperazin-1-yl]ethanesulfonic acid (HEPES) buffer (130 mM NaCl, 19.7 mM HEPES, 5 mM glucose, 5 mM KCl, 1.25 mM $CaCl_2$, 1.2 mM KH_2PO_4, 1 mM $MgSO_4$) and then with HEPES buffer supplemented with adenosine (500 μM) or ATP (100 μM). Dynamic changes in fluorescence intensity of perifused cells were live recorded using a 40× water objective. NIH ImageJ software[42] was used for post hoc analysis of live cell image series.

Histology and Fibrosis Scoring

A liver lobe of each animal was fixed overnight with 10% neutral-buffered formalin, dehydrated with 100% ethanol, and embedded in paraffin. Liver sections (5 μm thick) were further processed for deparaffinization. Hematoxylin and eosin, Pico Sirius red, and Masson trichrome staining procedures were performed by the Experimental Pathology Core Laboratory at UAMS. Low-power field (LPF) images (20×) were taken using a BX51 Olympus microscope (Olympus). Liver fibrosis stages were assessed using the METAVIR fibrosis scoring system[43] in a blinded manner.

Immunohistochemistry, Ki-67 Proliferation Index, Apoptosis Detection, and $CK19^+$ Cell Count

A liver lobe from each animal was fixed overnight with 10% neutral-buffered formalin, dehydrated with 100% ethanol, and embedded in paraffin. Liver sections (5 μm thick) were further processed for deparaffinization and subjected to heat-induced antigen retrieval with citrate buffer (pH 6.0) before permeabilization with 0.1% Triton X-100 in 1× PBS for 10 min. Nonspecific binding was prevented by incubation with a blocking solution of 7% horse serum and 0.5% BSA in 1× PBS for 1 h. Primary antibodies were diluted in the blocking solution for overnight incubation at 4°C. The next day, endogenous peroxidase/avidin/biotin blocking steps were performed prior to the addition of a biotin-conjugated donkey anti-rabbit or anti-rat IgG secondary antibody (Jackson Immunoresearch, West Grove, PA, USA) incubated at room temperature for 1 h. Detection was performed using the Vectastain Elite ABC System (Vector Laboratories, Burlingame, CA, USA) with the ImmPACT DAB peroxidase substrate (Vector Laboratories) according to the manufacturer's instructions. Sections were counterstained with aqueous hematoxylin (Accurate Chemical and Scientific Corporation, Westbury, NY, USA) and mounted with a Mowiol-based mounting media.

Apoptotic cells were detected using the TACS-XL In Situ Apoptosis Detection Kit–DAB following the manufacturer's instruction (Trevigen Inc., Gaithersburg, MD, USA).

Sections were imaged with an Axiovert Imager Z1 (Zeiss) or a BX51 Olympus microscope (Olympus). $Ki\text{-}67^+$ staining was determined on five random fields (100×) per tissue section using the NIH's ImageJ software and expressed as percentage of positive pixels per field. $CK19^+$ structures were counted on five random fields (100×) per tissue sections.

Statistical Analysis

Data are presented as the mean ± SEM. One-way ANOVA with the Bonferroni post hoc test was used for statistical analysis.

RESULTS

Normal H69 Cholangiocytes Express Functional A2bAR mRNA and Proteins

The first step to establish whether extracellular adenosine can modulate cholangiocyte physiology was to determine the expression profile of adenosine receptor(s) in H69 cholangiocytes, which physiologically mimic normal cholangiocytes. RT-PCR experiments using specific sets of primers (see Table 1) for each adenosine receptor were performed. As seen in Figure 1A and previously reported by our group[44], H69 cholangiocytes primarily express *ADORA2b* mRNA. Weak mRNA expression of *ADORA1*, *ADORA2a*, and *ADORA3*, splice variants 1 or 3, can also be observed. Only *ADORA3* variant 2 was not expressed (data not shown). Immunofluorescence experiments using a specific antibody against human A2bAR

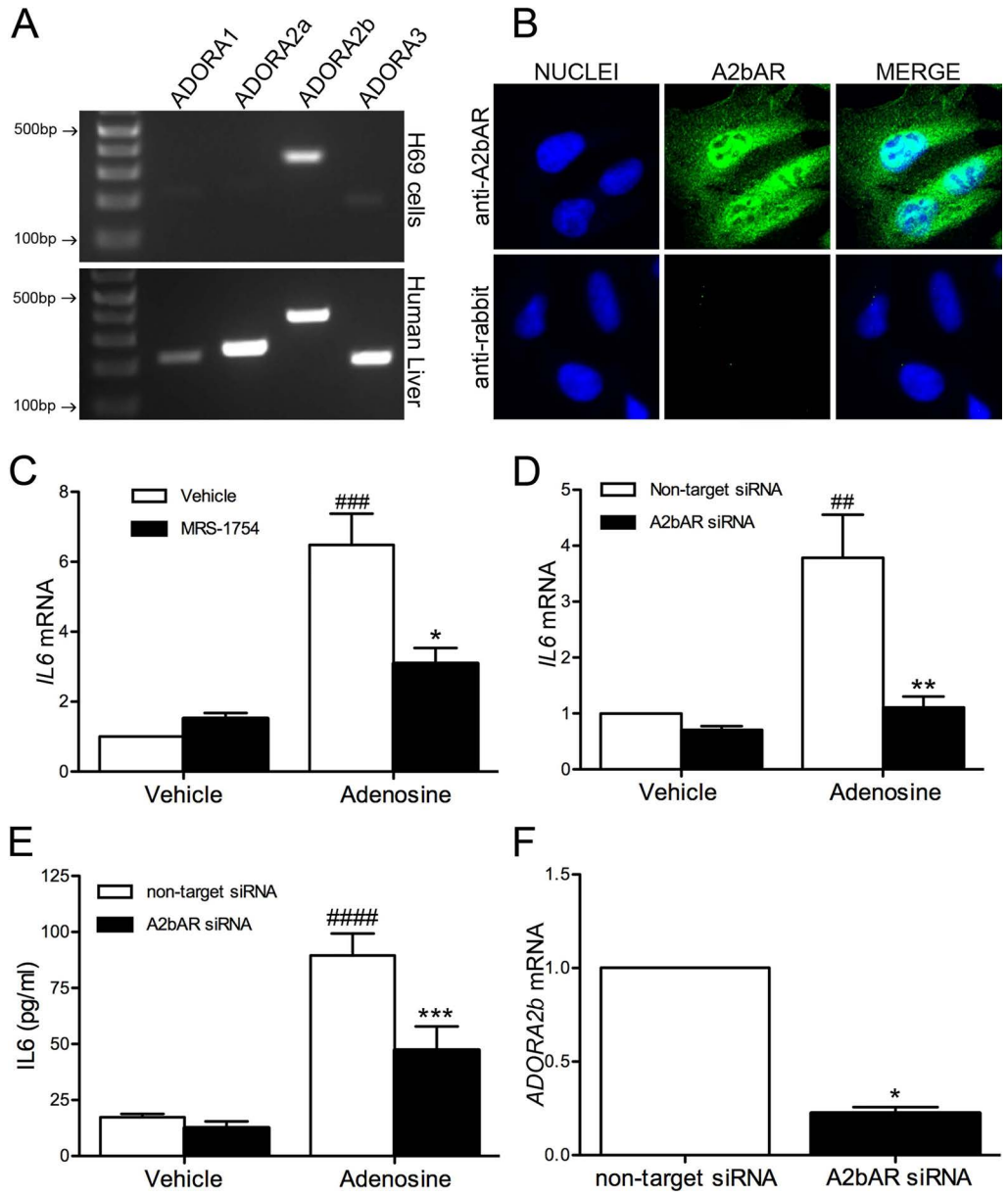

Figure 1. Adenosine induced interleukin-6 (IL-6) expression and secretion via the A2b adenosine receptor (A2bAR) in H69 cholangiocyte cells. (A) Reverse transcription polymerase chain reaction (RT-PCR) experiments were performed on complementary DNA (cDNA) extracted from H69 cholangiocyte cells using specific primers for each adenosine receptor isoforms (as listed in Table 1). Agarose gel (2%) electrophoresis with ethidium bromide staining was used to visualize the PCR products. Human liver cDNA was used as a positive control. The expected molecular weight PCR products were observed in the positive control. (B) Immunofluorescence staining of H69 cells with human A2bAR-specific antibody (anti-A2bAR) or anti-rabbit secondary antibody as negative control (anti-rabbit) confirmed that H69 cells express A2bAR at the protein level (green). Nuclei were stained with DAPI (blue). (C, D) H69 cells (150,000 cells per well in six-well plates) were stimulated with 100 μM adenosine for 2 h in complete media (C) in the presence of A2bAR antagonist MRS-1754 (1 μM; $n=6$) or (D) 72 h after transfection with A2bAR-specific siRNA ($n=5$). RNA was extracted, and IL-6 expression was assessed by qPCR using a specific probe for human IL-6 gene. β-2-microglobulin was used as a reference gene. #Significant when compared to the control without agonist; *significant when compared to vehicle (C) or nontarget siRNA (D). (E) H69 cells (30,000 cells per well in 48-well plates) were stimulated with 100 μM ADO for 4 h in 48-well plates in complete media 72 h after transfection with an A2bAR-specific siRNA. Supernatants were collected, centrifuged, and analyzed for IL-6 contents by ELISA. #Significant compared to the media alone; *significant compared to nontarget siRNA ($n=4$, performed in triplicate). (F) H69 cells were transfected with nontarget siRNA or A2bAR-specific siRNA with Lipofectamine 2000 for 72 h. RNA was extracted, and A2bAR expression was analyzed by qPCR using a human ADORA2b-specific probe. β-2-microglobulin was used as the gene of reference. *Significant when compared to nontarget siRNA ($n=8$).

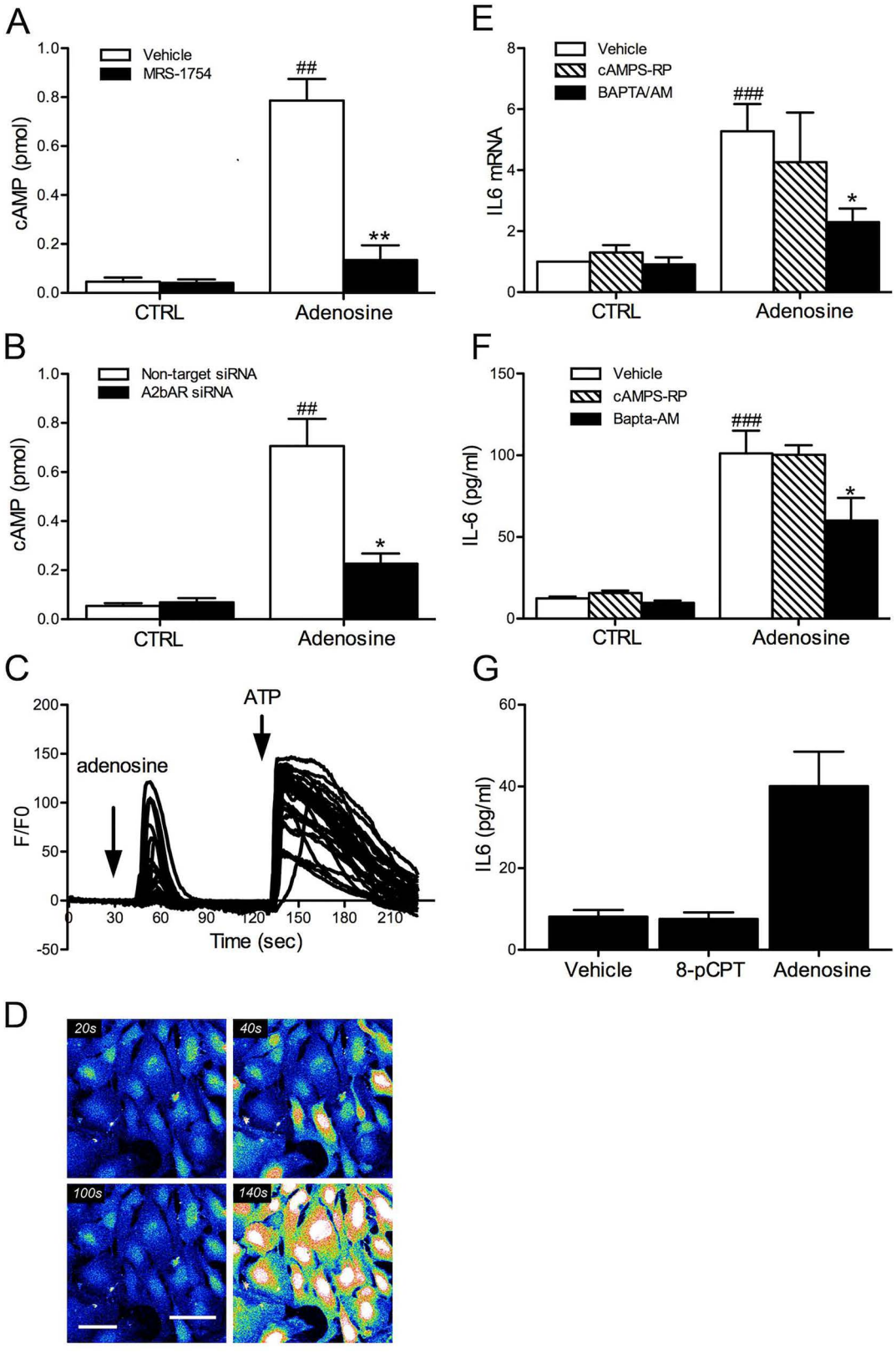
A
Vehicle
MRS-1754
cAMP (pmol)
1.0
0.8
0.6
0.4
0.2
0.0
##
**
CTRL
Adenosine
B
Non-target siRNA
A2bAR siRNA
cAMP (pmol)
1.0
0.8
0.6
0.4
0.2
0.0
##
*
CTRL
Adenosine
C
ATP
adenosine
F/F0
200
150
100
50
0
-50
0
30
60
90
120
150
180
210
Time (sec)
D
20s
40s
100s
140s
E
Vehicle
cAMPS-RP
BAPTA/AM
IL6 mRNA
8
6
4
2
0
###
*
CTRL
Adenosine
F
Vehicle
cAMPS-RP
Bapta-AM
IL-6 (pg/ml)
150
100
50
0
###
*
CTRL
Adenosine
G
IL6 (pg/ml)
60
40
20
0
Vehicle
8-pCPT
Adenosine

confirmed that H69 cholangiocytes do express A2bAR at the protein level (Fig. 1B).

Adenosine Stimulation of A2bAR Induces IL-6 Expression and Secretion in Normal H69 Cholangiocytes

Because A2bAR is a low-affinity receptor for adenosine[34], H69 cholangiocytes were stimulated with 100 μM of adenosine, a concentration known to activate A2bAR. Analysis of *IL-6* mRNA expression by qPCR shows an upregulation of 6.279±0.796-fold following a 2-h stimulation of H69 cholangiocytes with adenosine ligand (Fig. 1C). To confirm that the observed effect of adenosine was mediated by A2bAR, cells were also stimulated in the presence of MRS-1754, a selective A2bAR antagonist[41]. In the presence of MRS-1754, adenosine-induced *IL-6* mRNA upregulation was significantly reduced to 3.091±0.447 from 6.279±0.796-fold. H69 cholangiocytes were also transfected with specific A2bAR siRNA pools. A2bAR siRNAs downregulated the expression of the receptor by 77.52±3.241% after 72 h (Fig. 1F). In cells pretransfected with A2bAR siRNAs as seen in Figure 1D, no significant *IL-6* mRNA upregulation was observed following adenosine stimulation (1.108±0.197-fold), confirming that adenosine stimulation of the A2bAR mediates IL-6 mRNA upregulation in H69 cholangiocytes. Similar results were also obtained following stimulation of H69 cholangiocytes with 20 μM of NECA, a nonhydrolyzable and nonselective adenosine receptor agonist[45] (data not shown).

We then determined IL-6 protein release in response to adenosine (100 μM) in the supernatant of H69 cholangiocytes by ELISA. After 4 h of incubation with adenosine, 89.57±9.699 pg/ml of IL-6 was released. A specific A2bAR siRNA pool limited the IL-6 secretion to 47.23±10.63 pg/ml (Fig. 1E), confirming that this effect was mediated by A2bAR. Corresponding effects were observed with the A2bAR selective antagonist MRS-1754 (data not shown).

Pharmacological Analysis of A2bAR-Mediated Intracellular Signaling Pathways in Normal H69 Cholangiocytes

A2bAR is the only adenosine receptor known to signal via two distinct second messenger pathways, increasing cAMP concentration and mobilizing intracellular Ca^{2+} via G_s and G_q coupling, respectively[34]. Thus, we investigated which of these pathways is active in H69 cholangiocytes. Stimulation of H69 cholangiocytes by the AR receptor agonist adenosine activates the classic cAMP pathway, inducing an intracellular cAMP accumulation. A large decrease in cAMP accumulation was observed when H69 cholangiocytes are stimulated in the presence of the A2bAR selective antagonist MRS-1754, from 0.786±0.088 to 0.134±0.060 pmol/ml (Fig. 2A). Similar reductions were observed when H69 cells were pretransfected with an A2bAR siRNA (0.706±0.111 to 0.226±0.042 pmol/ml, respectively) (Fig. 2B), demonstrating that activation of A2bAR induced cAMP increases.

To assess the intracellular Ca^{2+} (Ca^{2+}_i) second messenger pathway, H69 cholangiocytes were preloaded with the calcium indicator fluorophore fluo-4/AM and perifused with adenosine (500 μM) in HEPES buffer. The result of a representative experiment is shown in Figure 2C and D. Adenosine induced a transient low-amplitude Ca^{2+}_i mobilization in H69 cells, in comparison with the more potent and long-lasting ATP mobilization, used as positive control. The peak intensity of the adenosine-induced intracellular Ca^{2+} mobilization varied from cell to cell compared to the effect of ATP (Fig. 2D). Taken together, these data show that both cAMP and Ca^{2+}_i A2bAR signaling pathways are functional in H69 cholangiocytes.

The next sets of experiments were performed to identify the pathway(s) involved in the modulation of

FACING PAGE

Figure 2. Second messenger alterations and control of IL-6 release mediated by adenosine/A2bAR. Intracellular cAMP concentrations (A, B) were analyzed by ELISA. H69 cells were stimulated with 100 μM adenosine for 2 h in 96-well plates (5,000 cells per well) in H69 complete media in the presence of A2bAR antagonist (A) MRS-1754 (1 μM; $n=3$, performed in triplicates) or (B) 72 h after transfection with an A2bAR-specific siRNA ($n=4$, performed in triplicate). #Significant when compared to the untreated cells; *significant when compared to vehicle (A) or nontarget siRNA (B). (C, D) Intracellular Ca^{2+} mobilization was observed by confocal microscopy. Glass coverslip-plated, fluo-4/AM-loaded H69 cells were perifused with HEPES buffer alone or containing 500 μM adenosine. ATP (100 μM) was used as a positive control. Changes in fluorescence intensity were recorded with a Zeiss 510 confocal microscope. (C) Relative fluorescence intensity of individual cells; 29 individual cells were analyzed. (D) Representative image of the dye intensity variation during the course of the experiment. Scale bar: 50 μm. (E) H69 cells were stimulated by 100 μM of adenosine for 2 h in six-well plates (150,000 cells per well) in H69 complete media. RNA was extracted, and IL-6 mRNA expression was determined by qPCR. Cells were preincubated with BAPTA/AM (50 μM) or cAMPs-RP (100 μM) 30 min prior to the stimulation ($n=3$ for cAMPs-RP and $n=7$ for BAPTA/AM). (F) H69 cells were stimulated by 100 μM adenosine for 4 h in 48-well plates (30,000 cells per well) in H69 complete media. Cells were preincubated with BAPTA/AM (50 μM) or cAMPs-RP (100 μM) 30 min prior to the stimulation. Supernatants were collected and centrifuged, and IL-6 content was analyzed by ELISA ($n=3$, performed in triplicate). #Significant when compared to unstimulated cells; *significant when compared to vehicle. (G) H69 cells were stimulated by 100 μM of 8-pCPT-2-O-Me-cAMP-AM (8-pCPT) or adenosine for 4 h in 48-well plates (30,000 cells per well) in H69 complete media. Supernatants were collected and centrifuged, and IL-6 content was analyzed by ELISA ($n=3$, performed in triplicate).

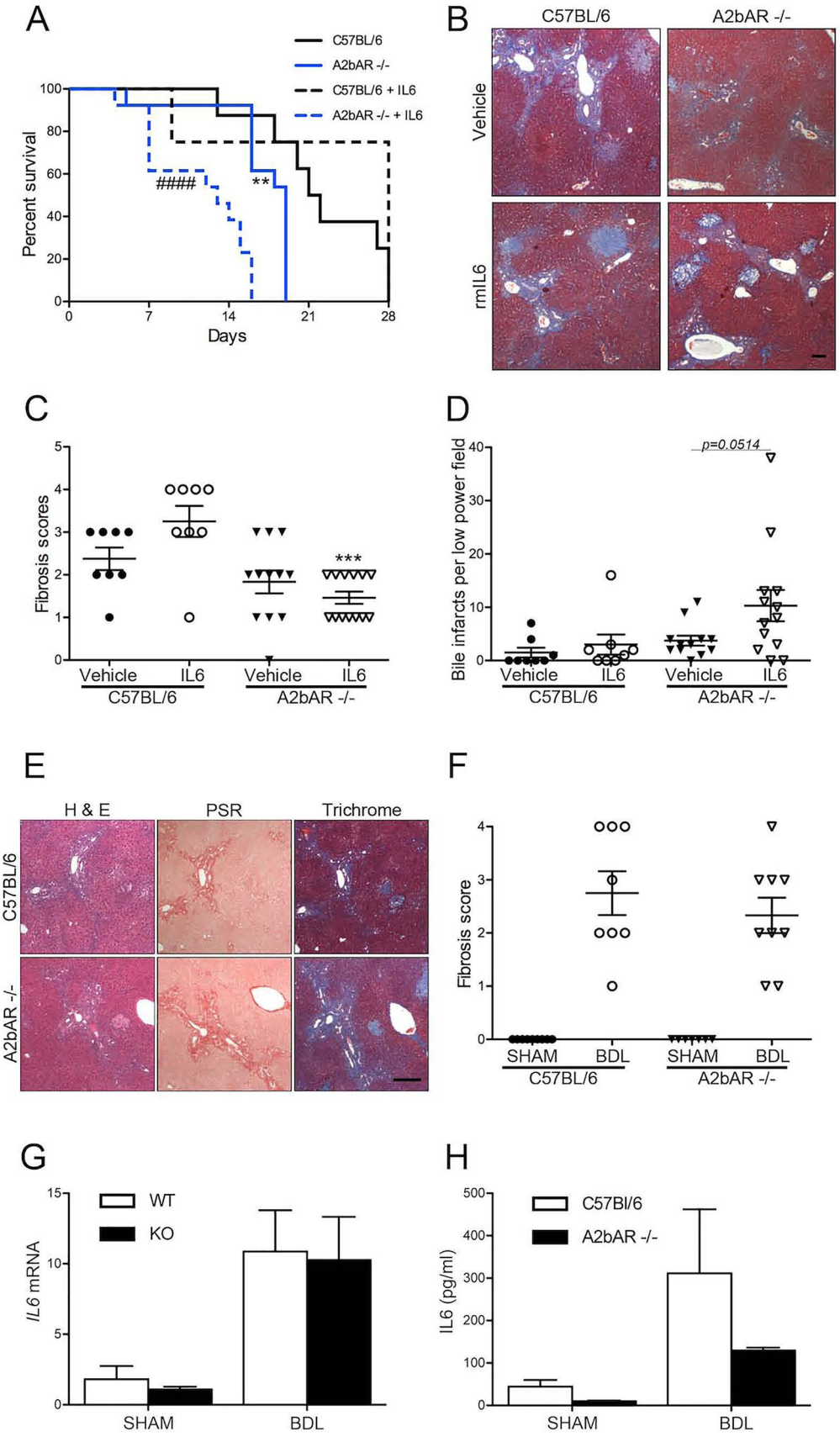
A
C57BL/6
A2bAR -/-
C57BL/6 + IL6
A2bAR -/- + IL6
Percent survival
Days
####
**
B
C57BL/6
A2bAR -/-
Vehicle
rmIL6
C
Fibrosis scores
Vehicle
IL6
Vehicle
IL6
C57BL/6
A2bAR -/-
***
D
Bile infarcts per low power field
p=0.0514
Vehicle
IL6
Vehicle
IL6
C57BL/6
A2bAR -/-
E
H & E
PSR
Trichrome
C57BL/6
A2bAR -/-
F
Fibrosis score
SHAM
BDL
SHAM
BDL
C57BL/6
A2bAR -/-
G
IL6 mRNA
WT
KO
SHAM
BDL
H
IL6 (pg/ml)
C57Bl/6
A2bAR -/-
SHAM
BDL

the IL-6 expression and protein secretion via a pharmacological approach. H69 cholangiocytes were incubated with adenosine in the presence of BAPTA/AM, an intracellular calcium chelator[46], or in presence of cAMPS-RP, an antagonist of the protein kinase A (PKA) downstream cAMP signaling[47]. IL-6 mRNA expression and secretion were analyzed, as shown in Figure 2E and F, respectively. In the presence of the calcium chelator BAPTA/AM, adenosine-induced IL-6 mRNA expression was significantly reduced (Fig. 2E). A similar tendency was observed for IL-6 secretion (Fig. 2F). In contrast, no effect of the cAMP-dependent protein kinase inhibitor cAMPS-RP was observed (Fig. 2E and F). As cAMP can also effect downstream changes by activating EPAC, H69 cholangiocytes were stimulated with 8-pCPT-2-O-Me-cAMP-AM, a specific EPAC activator, and IL-6 protein secretion was measured. As can be seen in Figure 2G, 8-pCPT-2-O-Me-cAMP-AM did not stimulate IL-6 secretion by H69 cells. Similar results were obtained when IL-6 mRNA expression was analyzed (data not shown). The data obtained strongly suggest that adenosine-mediated IL-6 expression/secretion by normal H69 cholangiocytes is dependent on an intracellular signaling pathway involving intracellular Ca^{2+} mobilization.

A2bAR Deficiency Increases Mortality and Alters the Ductular Reaction But Has no Effect on Biliary Cirrhosis Mediated by BDL

To determine the effect of A2bAR-mediated IL-6 release in biliary cirrhosis, we assessed the effect of A2bAR deficiency after bile duct ligation or sham surgery. IL-6-deficient mice were previously reported, in a 12-week BDL study, to have higher bilirubin and mortality rates than control littermates[15]. We thus performed a similar survival experiment with the A2bAR$^{-/-}$ mice. As observed in Figure 3A, the A2bAR$^{-/-}$ mice were significantly more susceptible to death after BDL than C57BL/6 control mice, with a median survival of 19 and 21.5 days, respectively. To assess whether the difference in mortality observed could be abolished by supplementation with exogenous IL-6, we tested mice weekly injected before surgery and thereafter with recmIL-6 (250 ng/g of body weight). The exogenous injection of IL-6 had no effect on the C57BL/6 control survival rate. However, A2bAR$^{-/-}$ mice injected with recmIL-6 showed markedly worsened survival after BDL, with a median survival of only 13 days compared to 19 days for the A2bAR$^{-/-}$ group injected with vehicle only. It is important to note that for the BDL survival experiment, since no A2bAR-deficient mice survived past 21 days, we made the decision to observe the C57BL/6 mice for a maximum of 28 days.

Histological analyses were performed on liver sections collected at sacrifice or shortly after the mice were found dead to determine the fibrotic stage (Fig. 3B and C). Masson trichrome-stained sections (Fig. 3B) were staged blindly using the METAVIR fibrosis scoring system. As observed in Figure 3C, A2bAR$^{-/-}$ mice had the same level of liver fibrosis at the time of death compared to the control C57BL/6 mice. Moreover, recmIL-6 injection had no effect on the fibrosis score, although there was a trend toward increased fibrosis in control wild-type mice receiving recombinant IL-6, and a significant difference is observed between these animals and the A2bAR-deficient animals that received IL-6 injection (3.250 ± 0.366 and 1.462 ± 0.144, respectively). These data suggest that A2bAR deficiency and exogenous IL-6 injection do not increase fibrosis development in BDL despite an evident effect in survival. One interesting observation was made in the hematoxylin and eosin low-power field staining (not shown). A nearly significant ($p = 0.0514$) increase in the number of bile infarcts was observed when exogenous IL-6 is injected to A2bAR-deficient mice (Fig. 3D).

To extend the results obtained with the survival experiment, a second group of mice were subjected to sham or BDL operation for a total of 2 weeks, since survival was consistent at this time point. Histological staining was performed as described above. Low-power field (20×) representative pictures are shown in Figure 3E. Blinded

FACING PAGE

Figure 3. Effect of A2bAR knockout on survival and fibrosis after bile duct ligation (BDL). BDL was performed on 10- to 12-week-old male C57BL/6 or A2bAR$^{-/-}$ mice. (A–D) A group of mice received weekly subcutaneous injection of recombinant mouse IL-6 (IL-6; $n = 13$ for both background), and the other group received vehicle only ($n = 8$ for both background). (A) Kaplan–Meier survival graph. The black line represents control C57BL/6 mice, and the blue line corresponds to A2bAR$^{-/-}$ mice. Full lines are vehicle only, and dotted lines represent mice that received recmIL-6 injections. *Significant when compared to C57BL/6 mice; #significant when compared to vehicle injection. (B) Mason trichrome staining representative of each group at the median time of survival. Scale bar: 100 μm. (C) METAVIR fibrosis score analysis of the Mason trichrome staining performed in a blinded manner. (D) Bile infarcts were counted on a blinded manner on low-power field hematoxylin and eosin staining of each individual mouse. (E–H) BDL or sham operation was performed on 10- to 12-week-old male C57BL/6 ($n = 9$ and 7, respectively) or A2bAR$^{-/-}$ mice ($n = 13$ and 7, respectively). Mice were sacrificed 2 weeks after surgery. (E) Representative picture of hematoxylin and eosin (H&E), Pico Sirius red (PSR), and Mason trichrome staining for each group of mice. Scale bar: 100 μm. (F) METAVIR fibrosis score analysis of the Mason trichrome staining performed in a blinded manner. (G) Total liver RNA was extracted, and relative *IL-6* mRNA was assessed by qPCR. *GAPDH*-specific probe was used as control. C57BL/6 and A2bAR$^{-/-}$ sham operated levels were, respectively, used as reference for the BDL group. (H) Serum was obtained from sham and BDL-operated mice, and total serum IL-6 was assessed by ELISA.

fibrosis scores, determined using the METAVIR scoring system, are presented in Figure 3F. As seen, no differences were observed for the fibrotic score between the A2bAR-deficient mice and the control wild-type mice 2 weeks after BDL surgery. The total liver *IL-6* mRNA level was determined by qPCR 2 weeks after BDL surgery, as shown in Figure 3G. *IL-6* mRNA is increased after BDL, but no variation is observed between groups from different genetic backgrounds. However, when serum IL-6 was assessed by ELISA 2 weeks after BDL, a nonsignificant reduction was observed for both sham and BDL-operated animals (Fig. 3H) when comparing C57BL/6 and A2bAR$^{-/-}$.

One of the key components of the ductular reaction in biliary fibrosis is cholangiocyte proliferation and ductular morphogenesis. To assess this, CK19 staining was performed on 2 week sham and BDL-operated animals that received or not weekly injection of recmIL-6. Representative images are shown in Figure 4A. The number of mature duct (showing a clear lumen) and nonduct (solitary or bunched cells without an organized lumen and duct structure) CK19^{+} cells was counted in a blinded fashion. Two weeks after BDL, A2bAR-deficient mice displayed significantly more mature ducts per portal area (Fig. 4B) than control wild-type mice, 17.43±1.468 and 10.65±0.7852, respectively. Interestingly, this significant increase in mature ducts was abolished by exogenous IL-6 injection, where the numbers were comparable to the C57BL/6 control animals (11.030±1.202 ducts/portal area). However, sham-operated A2bAR$^{-/-}$ mice had significantly more CK19^{+} nonduct cells per portal area than the control wild-type mice (14.27±1.578 vs. 4.567± 0.4988, respectively), as seen in Figure 4C. Following bile duct ligation, the number of nonduct CK19^{+} cells in the deficient mice decreased to reach the level of the control wild-type mice. The effect of exogenous IL-6 injection was surprising. As observed in Figure 4C, exogenous IL-6 injection significantly increased the number of nonduct CK19^{+} structures for the C57BL/6 sham-operated animals (4.241±0.537 vs. 13.300±1.345, respectively) but has no effect on the A2bAR$^{-/-}$ mice. As IL-6 is known to promote cell proliferation, Ki-67 staining was performed by immunohistochemistry, and the liver epithelial proliferation was expressed by percentage of positive staining analyzed with ImageJ software. As expected, a significant proliferation increase was observed for the C57BL/6 animals that received weekly injection of recombinant mouse IL-6 compared to the vehicle-injected animals (1.404±0.101 vs. 0.583±0.0813, respectively). However, when the A2bAR$^{-/-}$ mice were analyzed, no effect of exogenous IL-6 on cell proliferation was observed.

In an attempt to better understand the effect of the A2bAR deficiency and exogenous IL-6 observed on survival, staining for various inflammatory cells was performed. Neutrophils, macrophages, and T lymphocytes were stained using specific antibodies described in the Materials and Methods section; however, no effect of A2bAR deficiency and/or exogenous IL-6 treatment was observed on the number of infiltrating inflammatory cells (data not shown). In addition, a TUNEL assay performed to detect apoptotic cells showed no effect of A2bAR deficiency and/or exogenous IL-6 treatment (data not shown).

Taken together, these data suggest that the A2bAR/IL-6 pathway is important in ductular proliferation and morphogenesis following bile duct ligation and that this is independent of fibrosis but affect the survival capacity of the mice.

DISCUSSION

Cirrhosis is the end stage of chronic injury in the liver. Although progression of fibrosis is essential to the pathogenesis of cirrhosis, regeneration is equally necessary for cirrhosis to be present[48]. Although elegant studies focusing on fibrosis-regulating factors have elucidated relevant pathways, far fewer have examined regeneration, especially in the context of cirrhosis. Furthermore, regeneration is the defining response to acute liver injury, yet its mechanisms are similarly underevaluated in this context. We have tried to bridge this gap via the experiments performed in this article.

We focused on the mechanisms regulating IL-6 response at the cholangiocyte level for several reasons. First, excellent studies suggest that IL-6 is particularly relevant in both liver regeneration and biliary cirrhosis[10–15]. Second, our preliminary data showed that cholangiocytes release IL-6 in a regulated fashion[19]. Third, cholangiocytes are critical mediators in the pathogenesis of biliary cirrhosis[49]. Finally, the ectoenzyme cascade resulting in the generation of extracellular adenosine is altered in a fashion that favors increased extracellular adenosine content during liver fibrosis[36].

Our in vitro experiments show that adenosine induces IL-6 release form cholangiocytes via the A2bAR. This is intriguing for several reasons. Unlike the other adenosine receptors, A2bAR is a low-affinity receptor, suggesting that it may be of particular importance in liver response to injury, especially when massive amounts of ATP are released after cell death[50]. Moreover, in cells outside the liver, A2bAR has been linked to IL-6 release[22–24]. Data from our lab show that ATP-dependent IL-6 regulation in cholangiocytes is controlled by several Ca^{2+}/cAMP response elements (CRE) on the IL-6 promoter[19]. CRE has been shown to be activated by both Ca^{2+} and cAMP signals. While stimulation of A2bAR did induce cAMP and Ca^{2+} signals in this study, only the Ca^{2+} signals regulated IL-6 release. This suggests that, in this context, Ca^{2+} and not cAMP may be the primary effector of the

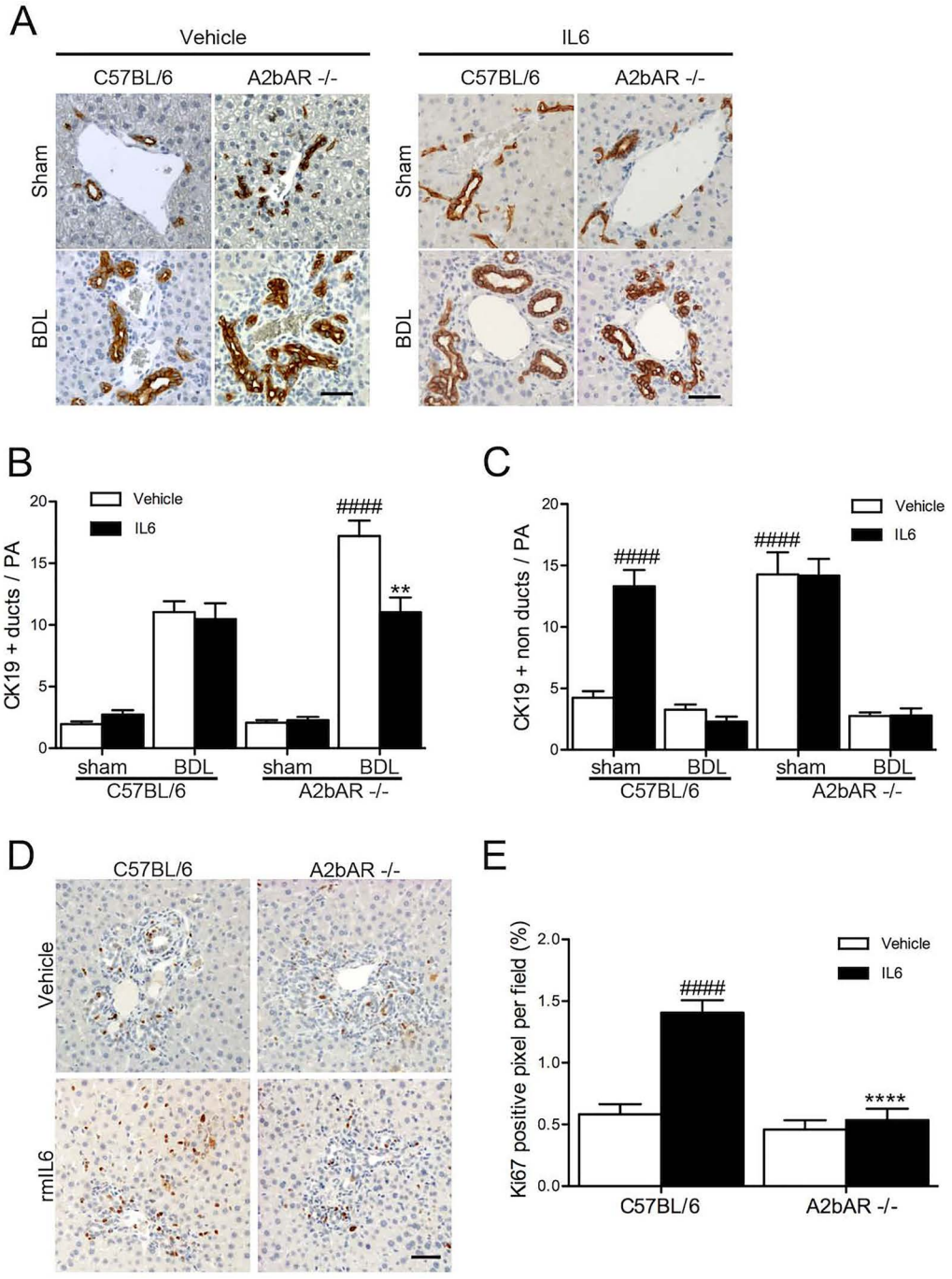

Figure 4. Bile duct staining with CK19 (A–C) and cell proliferation analysis by Ki-67 staining (D, E) were performed 2 weeks after BDL mice. A group of mice received recombinant mouse IL-6 (IL-6) or the vehicle only (vehicle) for both sham and BDL surgeries. (A) Representative CK19 staining image for each group. Scale bar: 50 μm. (D, E) Count of $CK19^{+}$ duct (D; with visible lumen) and nonduct (E; no lumen) per portal area in a blinded manner. The following were the number of animals per group: C57BL/6 sham (7), C57BL/6 sham + IL-6 (3), C57BL/6 BDL (9), C57BL/6 BDL + IL-6 (3), $A2bAR^{-/-}$ sham (7), $A2bAR^{-/-}$ sham + IL-6 (3), $A2bAR^{-/-}$ BDL (13), and $A2bAR^{-/-}$ BDL + IL-6 (3). Between 3 and 5 100× magnification fields were count per animal. #Significant when compared to C57BL/6 BDL vehicle; *significant when compared to $A2bAR^{-/-}$ BDL vehicle. (D) Representative image of Ki-67 staining for BDL-operated animal with or without recmIL-6 injection. Scale bar: 50 μm. (E) Analysis of the percent of $Ki\text{-}67^{+}$ pixels on five different 100× magnification fields for three animals per group. #Significant when compared to C57BL/6 BDL vehicle; *significant when compared to C57BL/6 BDL IL-6.

A2bAR. Of note, similar results were observed with A2bAR-mediated IL-6 released by dendritic cells[24] and by macrophages and endothelial cells[51], providing support for this provocative finding.

The results obtained in vivo after bile duct ligation were particularly surprising in light of published studies. These studies presumed that poor survival in the absence of IL-6 was due to differences in the rate of fibrosis/cirrhosis progression[15]. Here we show that this is not the case. The A2bAR-deficient mice died prematurely, and this was worsened by exogenous recmIL-6. However, the fibrosis scores at the time of death were unchanged in such mice. At this time, the mechanisms increasing mortality in these animals are unknown. However, the presence of bile infarcts in animals with increased mortality due to recombinant IL-6 injection (without observed changes in inflammatory cells) suggests that epithelial repair mechanisms may be of great importance. We are confident that the mortality difference is not due to changes in fibrosis because at the 2-week time point (when all animals were alive) fibrosis progression was identical. In contrast, the character of the ductular reaction was altered in A2bAR-deficient mice. Specifically, BDL induced a greater shift from nonduct to duct-forming cholangiocytes in mice lacking A2bAR, suggesting that IL-6 may push cholangiocytes to a pluripotential, proliferative phenotype as opposed to a secretory, reactive phenotype, as observed by Alpini and colleagues in the setting of cholangiocyte size–phenotype correlation[52]. Furthermore, observations at the 2-week time point indicate that A2bAR-deficient mice lack a response to recombinant IL-6 that is robust in wild-type mice. We propose that IL-6 is relevant to repair and ductular morphogenesis, but cholangiocytes unable to generate IL-6 in response to extracellular adenosine lose this regulatory mechanism. The specific cause of this alteration is, at this time, unknown but should be investigated in future studies.

Three other points are worth mentioning, although there are insufficient data to explain them fully at this time. First, the mechanism by which IL-6 increases mortality in our model may not be due to physiological effects of IL-6 but rather the effects of supratherapeutic administration of IL-6. In other words, a large bolus dose of IL-6 may activate mechanisms not yet defined, which ultimately impair survival. Although outside of the scope of this article, this is worth further study. Second, although the in vitro segment of this study was designed to examine the cholangiocyte adenosine/A2b/IL-6 axis, the in vivo work involved whole-animal knockouts. Thus, the specific role of cholangiocyte IL-6 release in vivo could not be studied in isolation. The roles of other cells with relevant adenosine/A2b pathways may have skewed our in vivo findings. Again, future studies should address this question. Last, the cholangiocyte adenosine/A2b axis, even if it does mediate regulated release of IL-6, may also regulate release of other inflammatory mediators. We have investigated this at a preliminary level, but the data were equivocal. That said, since we have characterized both cAMP and cytosolic Ca^{2+} as downstream effectors of A2b, it is almost certain that adenosine regulates functions in addition to IL-6 release in cholangiocytes. All of these considerations are important in the evaluation of the data presented in this article.

In summary, we describe a novel pathway that relates regenerative injury and survival in biliary cirrhosis. This pathway, mediated by extracellular adenosine, the A2bAR, Ca^{2+}, and IL-6, merits further experimental study, with hopes of generating a more complete understanding of the response of the liver to acute and chronic injury.

ACKNOWLEDGMENTS: Author roles: E. G. Lavoie (performance or supervision of all experiments and authorship of the manuscript first draft and revisions); M. Fausther (oversight and review of the manuscript); J. R. Goree (performance of the key experiments); J. A. Dranoff (experimental design, manuscript revision, and authorship). The authors declare no conflicts of interest.

REFERENCES

1. Mao SA, Glorioso JM, Nyberg SL. Liver regeneration. Transl Res. 2014;163:352–62.
2. Fausto N. Liver regeneration. J Hepatol. 2000;32:19–31.
3. Drucker C, Gewiese J, Malchow S, Scheller J, Rose-John S. Impact of interleukin-6 classic- and trans-signaling on liver damage and regeneration. J Autoimmun. 2010;34:29–37.
4. Kishimoto T. Interleukin-6: From basic science to medicine—40 years in immunology. Annu Rev Immunol. 2005;23:1–21.
5. Wolf J, Rose-John S, Garbers C. Interleukin-6 and its receptors: A highly regulated and dynamic system. Cytokine 2014;70:11–20.
6. Tanaka T, Narazaki M, Kishimoto T. IL-6 in inflammation, immunity, and disease. Cold Spring Harb Perspect Biol. 2014;6:a016295.
7. Ramadori G, Christ B. Cytokines and the hepatic acute-phase response. Semin Liver Dis. 1999;19:141–55.
8. Camargo CA Jr, Madden JF, Gao W, Selvan RS, Clavien PA. Interleukin-6 protects liver against warm ischemia/reperfusion injury and promotes hepatocyte proliferation in the rodent. Hepatology 1997;26:1513–20.
9. Park J, Gores GJ, Patel T. Lipopolysaccharide induces cholangiocyte proliferation via an interleukin-6-mediated activation of p44/p42 mitogen-activated protein kinase. Hepatology 1999;29:1037–43.
10. Trautwein C, Rakemann T, Niehof M, Rose-John S, Manns MP. Acute-phase response factor, increased binding, and target gene transcription during liver regeneration. Gastroenterology 1996;110:1854–62.
11. Tachibana S, Zhang X, Ito K, Ota Y, Cameron AM, Williams GM, Sun Z. Interleukin-6 is required for cell cycle arrest and activation of DNA repair enzymes after partial hepatectomy in mice. Cell Biosci. 2014;4:6.
12. Cressman DE, Greenbaum LE, DeAngelis RA, Ciliberto G, Furth EE, Poli V, Taub R. Liver failure and defective hepatocyte regeneration in interleukin-6-deficient mice. Science 1996;274:1379–83.

13. Blindenbacher A, Wang X, Langer I, Savino R, Terracciano L, Heim MH. Interleukin 6 is important for survival after partial hepatectomy in mice. Hepatology 2003;38:674–82.
14. Sakamoto T, Liu Z, Murase N, Ezure T, Yokomuro S, Poli V, Demetris AJ. Mitosis and apoptosis in the liver of interleukin-6-deficient mice after partial hepatectomy. Hepatology 1999;29:403–11.
15. Ezure T, Sakamoto T, Tsuji H, Lunz JG 3rd, Murase N, Fung JJ, Demetris AJ. The development and compensation of biliary cirrhosis in interleukin-6-deficient mice. Am J Pathol. 2000;156:1627–39.
16. Gregory SH, Wing EJ, Danowski KL, van Rooijen N, Dyer KF, Tweardy DJ. IL-6 produced by Kupffer cells induces STAT protein activation in hepatocytes early during the course of systemic listerial infections. J Immunol. 1998;160:6056–61.
17. Nieto N. Ethanol and fish oil induce NFkappaB transactivation of the collagen alpha2(I) promoter through lipid peroxidation-driven activation of the PKC-PI3K-Akt pathway. Hepatology 2007;45:1433–45.
18. Kawasaki T, Murata S, Takahashi K, Nozaki R, Ohshiro Y, Ikeda N, Pak S, Myronovych A, Hisakura K, Fukunaga K, Oda T, Sasaki R, Ohkohchi N. Activation of human liver sinusoidal endothelial cell by human platelets induces hepatocyte proliferation. J Hepatol. 2010;53:648–54.
19. Yu J, Sheung N, Soliman EM, Spirli C, Dranoff JA. Transcriptional regulation of IL-6 in bile duct epithelia by extracellular ATP. Am J Physiol Gastrointest Liver Physiol. 2009;296:G563–71.
20. O'Hara SP, Splinter PL, Trussoni CE, Gajdos GB, Lineswala PN, LaRusso NF. Cholangiocyte N-Ras protein mediates lipopolysaccharide-induced interleukin 6 secretion and proliferation. J Biol Chem. 2011;286:30352–60.
21. Isse K, Specht SM, Lunz JG 3rd, Kang LI, Mizuguchi Y, Demetris AJ. Estrogen stimulates female biliary epithelial cell interleukin-6 expression in mice and humans. Hepatology 2010;51:869–80.
22. Schwaninger M, Neher M, Viegas E, Schneider A, Spranger M. Stimulation of interleukin-6 secretion and gene transcription in primary astrocytes by adenosine. J Neurochem. 1997;69:1145–50.
23. Sitaraman SV, Merlin D, Wang L, Wong M, Gewirtz AT, Si-Tahar M, Madara JL. Neutrophil-epithelial crosstalk at the intestinal lumenal surface mediated by reciprocal secretion of adenosine and IL-6. J Clin Invest. 2001;107:861–9.
24. Wei W, Du C, Lv J, Zhao G, Li Z, Wu Z, Haskó G, Xie X. Blocking A2B adenosine receptor alleviates pathogenesis of experimental autoimmune encephalomyelitis via inhibition of IL-6 production and Th17 differentiation. J Immunol. 2013;190:138–46.
25. Corriden R, Insel PA. Basal release of ATP: An autocrine-paracrine mechanism for cell regulation. Sci Signal. 2010; 3:re1.
26. Hasko G, Cronstein BN. Adenosine: An endogenous regulator of innate immunity. Trends Immunol. 2004;25:33–9.
27. Fredholm BB. Adenosine, an endogenous distress signal, modulates tissue damage and repair. Cell Death Differ. 2007; 14:1315–23.
28. Chan ES, Cronstein BN. Adenosine in fibrosis. Mod Rheumatol. 2010;20:114–22.
29. Knowles AF. The GDA1_CD39 superfamily: NTPDases with diverse functions. Purinergic Signal. 2011;7:21–45.
30. Robson SC, Sevigny J, Zimmermann H. The E-NTPDase family of ectonucleotidases: Structure function relationships and pathophysiological significance. Purinergic Signal. 2006;2:409–30.
31. Zimmermann H, Zebisch M, Strater N. Cellular function and molecular structure of ecto-nucleotidases. Purinergic Signal. 2012;8:437–502.
32. Jacobson KA, Gao ZG. Adenosine receptors as therapeutic targets. Nat Rev Drug Discov. 2006;5:247–64.
33. Jacobson KA. Introduction to adenosine receptors as therapeutic targets. Handb Exp Pharmacol. 2009:1–24.
34. Linden J, Thai T, Figler H, Jin X, Robeva AS. Characterization of human A(2B) adenosine receptors: Radioligand binding, Western blotting, and coupling to G(q) in human embryonic kidney 293 cells and HMC-1 mast cells. Mol Pharmacol. 1999;56:705–13.
35. Fausther M, Lecka J, Soliman E, Kauffenstein G, Pelletier J, Sheung N, Dranoff JA, Sévigny J. Coexpression of ecto-5′-nucleotidase/CD73 with specific NTPDases differentially regulates adenosine formation in the rat liver. Am J Physiol Gastrointest Liver Physiol. 2012;302:G447–59.
36. Fausther M, Sheung N, Saiman Y, Bansal MB, Dranoff JA. Activated hepatic stellate cells upregulate transcription of ecto-5′-nucleotidase/CD73 via specific SP1 and SMAD promoter elements. Am J Physiol Gastrointest Liver Physiol. 2012;303:G904–14.
37. Yang D, Zhang Y, Nguyen HG, Koupenova M, Chauhan AK, Makitalo M, Jones MR, St Hilaire C, Seldin DC, Toselli P, Lamperti E, Schreiber BM, Gavras H, Wagner DD, Ravid K. The A2B adenosine receptor protects against inflammation and excessive vascular adhesion. J Clin Invest. 2006;116:1913–23.
38. Miyoshi H, Rust C, Roberts PJ, Burgart LJ, Gores GJ. Hepatocyte apoptosis after bile duct ligation in the mouse involves Fas. Gastroenterology 1999;117:669–77.
39. Grubman SA, Perrone RD, Lee DW, Murray SL, Rogers LC, Wolkoff LI, Mulberg AE, Cherington V, Jefferson DM. Regulation of intracellular pH by immortalized human intrahepatic biliary epithelial cell lines. Am J Physiol. 1994; 266:G1060–70.
40. Klotz KN. Adenosine receptors and their ligands. Naunyn Schmiedebergs Arch Pharmacol. 2000;362:382–91.
41. Kim YC, Ji X, Melman N, Linden J, Jacobson KA. Anilide derivatives of an 8-phenylxanthine carboxylic congener are highly potent and selective antagonists at human A(2B) adenosine receptors. J Med Chem. 2000;43:1165–72.
42. Schneider CA, Rasband WS, Eliceiri KW. NIH Image to ImageJ: 25 years of image analysis. Nat Methods 2012; 9:671–5.
43. Bedossa P, Poynard T. An algorithm for the grading of activity in chronic hepatitis C. The METAVIR Cooperative Study Group. Hepatology 1996;24:289–93.
44. Goree JR, Lavoie EG, Fausther M, Dranoff JA. Expression of mediators of purinergic signaling in human liver cell lines. Purinergic Signal. 2014;10:631–8.
45. Cusack NJ, Hourani SM. 5′-*N*-ethylcarboxamidoadenosine: A potent inhibitor of human platelet aggregation. Br J Pharmacol. 1981;72:443–7.
46. Raspe E, Ramboer I, Galand N, Boeynaems JM. Enhanced release of prostacyclin from quin 2-loaded endothelial cells. Eur J Pharmacol. 1989;163:345–51.
47. Van Haastert PJ, Van Driel R, Jastorff B, Baraniak J, Stec WJ, De Wit RJ. Competitive cAMP antagonists for cAMP-receptor proteins. J Biol Chem. 1984;259:10020–4.
48. Saffioti F, Pinzani M. Development and regression of cirrhosis. Dig Dis. 2016;34:374–81.

49. Lazaridis KN, LaRusso NF. The cholangiopathies. Mayo Clin Proc. 2015;90:791–800.
50. Gonzales E, Julien B, Serriere-Lanneau V, Nicou A, Doignon I, Lagoudakis L, Garcin I, Azoulay D, Duclos-Vallée JC, Castaing D, Samuel D, Hernandez-Garcia A, Awad SS, Combettes L, Thevananther S, Tordjmann T. ATP release after partial hepatectomy regulates liver regeneration in the rat. J Hepatol. 2010;52:54–62.
51. Figler RA, Wang G, Srinivasan S, Jung DY, Zhang Z, Pankow JS, Ravid K, Fredholm B, Hedrick CC, Rich SS, Kim JK, LaNoue KF, Linden J. Links between insulin resistance, adenosine A2B receptors, and inflammatory markers in mice and humans. Diabetes 2011;60:669–79.
52. Maroni L, Haibo B, Ray D, Zhou T, Wan Y, Meng F, Marzioni M, Alpini G. Functional and structural features of cholangiocytes in health and disease. Cell Mol Gastroenterol Hepatol. 2015;1:368–80.